# Capacitive Instrumentation and Sensor Fusion for High-Bandwidth Nanopositioning

Steven Ian Moore, Andrew J. Fleming and Yuen Kuan Yong

***Abstract*—Precision capacitive sensing methods encode the measurement in a high frequency signal which requires demodulation. To extract the measurement, the signal is observed over many cycles limiting the bandwidth of the sensor and introducing an undesirable phase lag. To address this limitation, this article outlines a design which fuses the output of a standard modulated capacitive sensor and a charge amplifier, providing an instantaneous capacitive measurement whose bandwidth is only limited by the speed at which the electronics operate.**

## I. Introduction

Sensor-based feedback control of piezoelectric nanopositioners is required to provide insensitivity to modeling errors and nonlinearities exhibited by piezoelectric ceramics [1]–[3]. Capacitive sensors are the most common type of instrumentation used in short range nanopositioning applications due to their linearity and resolution [4]. State-of-the-art capacitive sensors focus on high resolution measurements of static or pseudo-static capacitances where the measurement is encoded in the amplitude, phase, frequency, or mean of a high frequency signal that requires demodulation [5]. Demodulation is inherently a slow process where the output signal must be observed for many cycles. This ultimately limits the bandwidth – a high bandwidth is beneficial to sense fast dynamics and to minimize the dynamic error introduced due to the phase lag [4].

This article describes a capacitive sensor which fuses the measurement of a charge amplifier with that of a standard modulated capacitive sensor to provide a precise measurement over a bandwidth on the order of megahertz. Apart from nanopositioning, this sensor is suitable to observe fast dynamics in applications such as tomography [6] and in MEMS [7].

## II. Sensor Design

Two capacitive probes (MicroSense 2804) are used to observe the motion of a moving target via a varying capacitance $c(t)$. One probe is connected to a precision capacitive sensor (MicroSense 8810) which has a resolution of 1.5 nm–rms in a 1 kHz frequency band, however, the demodulation process limits its bandwidth. The second probe is connected to a charge amplifier which has a significantly higher bandwidth but cannot observe static motion. To address the limitations of each sensor, their outputs are fused together with the system shown in Figure 1.

The authors are with the School of Electrical Engineering and Computing, The University of Newcastle, Callaghan, NSW 2308, Australia (e-mail: steven.i.moore@uon.edu.au, andrew.fleming@newcastle.edu.au, yuenkuan.yong@newcastle.edu.au).

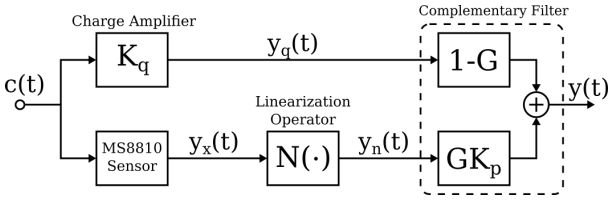


Fig. 1. Overview of the capacitive sensing system. The MS-8810 and the charge amplifier measure capacitive changes in mutually exclusive frequency bands. A complementary filter fuses the two signals together.

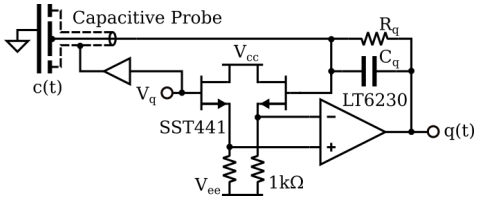


Fig. 2. The schematic of the charge amplifier. The op-amp is from Linear Technology and the dual JFET is from Linear Systems.

The dynamics of the charge amplifier, shown in Figure 2, are modeled by the transfer function

$$K_q(s) = \frac{Y_q(s)}{C(s)} = \frac{V_q R_q s}{C_q R_q s + 1}. \tag{1}$$

The parameters of the sensor are listed in Table I. The bandwidth of the charge amplifier was identified to be 13.41 MHz by replacing the capacitive probe with a charge source.

The MS-8810 is linear with respect to displacement and contains $F_x$, a second-order Butterworth filter with cutoff frequency $\omega_x$, to suppress demodulation artifacts. The output

TABLE I
Capacitive sensor parameters and characteristics.

| Parameter | Symbol | Value |
|---|---|---|
| Radius of the Capacitive Probe | $r$ | 1 mm |
| Standoff Distance | $x_0$ | 50 µm |
| MS-8810 Filter Natural Frequency | $\omega_x$ | 7929 rad/s |
| MS-8810 Gain | $k_x$ | 0.4 V/µm |
| Charge Amp. Feedback Resistor | $R_q$ | 10 GΩ |
| Charge Amp. Feedback Capacitor | $C_q$ | 0.5 pF |
| Charge Amp. Bias Voltage | $V_q$ | 5 V |
| MS8810 Input Noise Floor | $A_1$ | 19.13 µV$^2$/Hz |
| MS8810 Output Noise Floor | $A_2$ | 0.1632 µV$^2$/Hz |
| Charge Amp. Noise Floor | $A_3$ | 6.847 µV$^2$/Hz |
| Charge Amp. Noise Corner Freq. | $\omega_{nc}$ | 3057 rad/s |
| Natural Frequency of $F_p$ | $\omega_p$ | 62 569 rad/s (9958 Hz) |
| Natural Frequency of $G$ | $\omega_g$ | 1368 rad/s (218 Hz) |

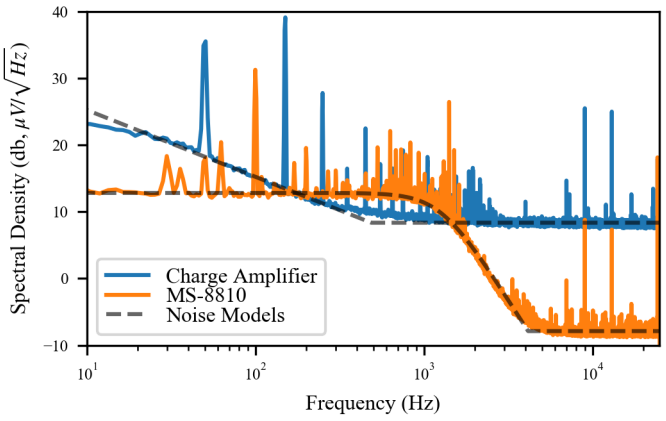


Fig. 3. The spectral density of the noise observed in the signals $y_x(t)$ and $y_q(t)$.

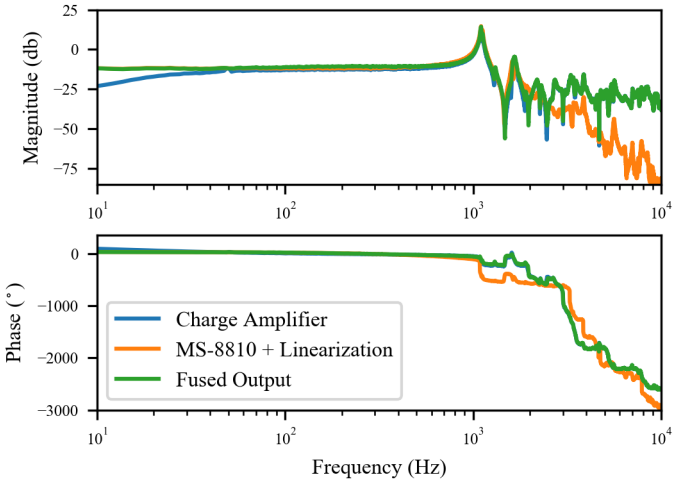


Fig. 4. The frequency response of the nanopositioning system from the amplifier input voltage to the charge amplifier output $y_q(t)$, linearized MS-8810 output $y_n(t)$, and the fused output $y(t)$. Portions of the charge amplifier and linearized MS-8810 response coincide with the fused output response.

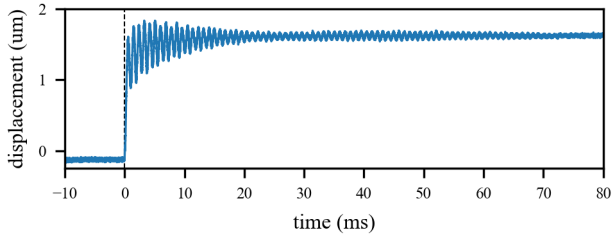


Fig. 5. The step response of the estimated displacement $y_d(t)$.

voltage of the MS-8810 is

$$y_x(t) = k_x F_x(s) \left( \frac{A\varepsilon}{c(t)} - x_0 \right), \tag{2}$$

where $A = \pi r^2$ is the area of the probe. Note $y(t) = F(s)u(t)$ is shorthand for $y(t) = f(t) * u(t)$, where $f(t) = \mathcal{L}^{-1}\{F(s)\}$. The sensor is linearized with the function

$$y_n(t) = N(y_x) = \frac{V_q k_x A\varepsilon}{C_q \left(k_x x_0 + y_x(t)\right)}. \tag{3}$$

The gain $V_q/C_q$ is applied to equate the gain in the passband to that of the charge amplifier. Equations (2) and (3) are are linearized at $C_0 = A\varepsilon/x_0$ as

$$K_x(s) = k_x \frac{A\varepsilon}{C_0^2} F_x(s), \qquad n_x = \frac{V_q C_0}{C_q k_x x_0}. \tag{4}$$

## III. Sensor Fusion

For cases where two sensors operate in mutually exclusive frequency bands, complementary filtering is an appropriate technique for sensor fusion [8]. Kalman filters, commonly used for sensor fusion, optimally minimize the difference between the fused output and the true sensor signal [9]. In comparison, complementary filters are not optimal but provide a simpler approach to design and implementation. The complementary filter in Figure 1 is comprised of

$$G(s) = \frac{\omega_g}{s + \omega_g}, \qquad K_p(s) = F_x^{-1}(s) F_p(s), \tag{5}$$

where $F_p$, a second-order Butterworth filter with cutoff frequency $\omega_p$, compensates for the dynamics of $F_x$. The sensor fusion parameters $\omega_g$ and $\omega_p$ are selected to minimize the mean noise squared of the capacitive measurement.

The power spectral density (PSD) of the noise on $y_q(t)$ and $y_x(t)$ are experimentally measured, shown in Figure 3, and the noise models

$$S_x(\omega) = A_1 |F_x(j\omega)|^2 + A_2, \tag{6}$$

$$S_q(\omega) = A_3 \frac{w_{nc}}{|\omega|} + A_3, \tag{7}$$

are fitted to the data. The PSD at the fused output is

$$S_y(\omega) = |G(j\omega) K_p(j\omega) n_x|^2 S_x(\omega) + |1 - G(j\omega)|^2 S_q(\omega). \tag{8}$$

Using the PSD, the mean noise squared of the capacitance measurement is

$$E(n^2) = \frac{1}{\pi} \int_{\omega_l}^{\omega_h} \frac{S_y(\omega)}{|K_y(j\omega)|^2} \, d\omega, \tag{9}$$

where $K_y$ is the linearized mapping from $c(t)$ to $y(t)$, that is

$$K_y(s) = (1 - G(s)) K_q(s) + G(s) K_p(s) K_x(s) n_x. \tag{10}$$

The integral is evaluated in the frequency band $0.01\,\text{Hz} - 1 \times 10^6\,\text{Hz}$. Optimization is used to minimize this equation to select $\omega_g$ and $\omega_p$. The identified noise parameters and the optimized sensor fusion parameters are listed in Table I.

## IV. Nanopositioning Application

The proposed capacitive instrumentation is tested on a nanopositioner (PI P-733.3DD) which is driven by an amplifier (PiezoDrive PDL200). The output of the capacitive sensor is converted back to displacement with

$$y_d(t) = \left( \frac{V_q A\varepsilon}{C_q y(t)} - x_0 \right). \tag{11}$$

Using a function generator, white noise excitation was applied to the amplifier driving the nanopositioner to identify the

frequency response of the system, shown in Figure 4. Like the MS-8810, the fused sensor is able to observe low frequency motion. As the frequency increases the fused response transitions to the charge amplifier. The magnitude response of the MS-8810 rolls off at high frequencies; only the charge amplifier operates at this bandwidth. The step response in Figure 5 shows the estimated displacement of the nanopositioner using the capacitive instrumentation demonstrating the suitability of the sensor for displacement instrumentation in nanopositioning.

## V. Conclusion

This article outlines a technique to increase the bandwidth of a capacitive sensor to a demonstrated bandwidth of 13.41 MHz. The simplicity of the fast sensor and the sensor fusion allow the design to be easily integrated with existing precision capacitive sensors to provide an increase in bandwidth.

## References


[1] S. O. R. Moheimani, "Invited review article: Accurate and fast nanopositioning with piezoelectric tube scanners: Emerging trends and future challenges," *Review of Scientific Instruments*, vol. 79, no. 7, p. , 2008.

[2] S. P. Wadikhaye, Y. K. Yong, B. Bhikkaji, and S. O. R. Moheimani, "Control of a piezoelectrically actuated high-speed serial-kinematic afm nanopositioner," *Smart Materials and Structures*, vol. 23, no. 2, p. 025030, 2014.

[3] Y. K. Yong and A. J. Fleming, "High-speed vertical positioning stage with integrated dual-sensor arrangement," *Sensors & Actuators: A. Physical*, vol. 248, pp. 184–192, 2016.

[4] A. J. Fleming, "A review of nanometer resolution position sensors: Operation and performance," *Sensors and Actuators A: Physical*, vol. 190, no. 0, pp. 106 – 126, 2013.

[5] L. K. Baxter, *Capacitive Sensors: Design and Application*. Wiley-IEEE Press, 1997.

[6] M. Demori, V. Ferrari, D. Strazza, and P. Poesio, "A capacitive sensor system for the analysis of two-phase flows of oil and conductive water," *Sensors and Actuators A: Physical*, vol. 163, no. 1, pp. 172 – 179, 2010.

[7] V. Kaajakari, *Practical MEMS*. Small Gear Publishing, 2009.

[8] W. T. Higgins, "A comparison of complementary and kalman filtering," *IEEE Transactions on Aerospace and Electronic Systems*, vol. AES-11, no. 3, pp. 321–325, 1975.

[9] R. G. Brown and P. Y. C. Hwang, *Introduction to Random Signals and Applied Filtering*. John Wiley & Sons, 2012.